BIOCHEMICAL PHARMACOLOGY 74 (2007) 557–565

available at www.sciencedirect.com

ScienceDirect

journal homepage: www.elsevier.com/locate/biochempharm

Apoptosis induction of 2′-hydroxycinnamaldehyde as a proteasome inhibitor is associated with ER stress and mitochondrial perturbation in cancer cells

Su Hyung Hong [a], *Jina Kim* [b], *Jung-Min Kim* [b], *So-Young Lee* [b], *Dae-Seop Shin* [b], *Kwang-Hee Son* [b], *Dong Cho Han* [b,**], *Young Kwan Sung* [c], *Byoung-Mog Kwon* [b,*]

[a] *Department of Dental Microbiology, School of Dentistry, Kyungpook National University, Daegu 700-412, Republic of Korea*
[b] *Korea Research Institute of Bioscience and Biotechnology, 52 Uendong Yoosung, Daejeon 305-600, Republic of Korea*
[c] *Department of Immunology, School of Medicine, Kyungpook National University, Daegu 700-422, Republic of Korea*

ARTICLE INFO

Article history:
Received 13 March 2007
Accepted 21 May 2007

Keywords:
2′-hydroxycinnamaldehyde
Apoptosis
Proteasome
Endoplasmic reticulum
Mitochondria

ABSTRACT

2′-Hydroxycinnamaldehyde (HCA), isolated from the stem bark of *Cinnamomum cassia*, and 2′-benzoyloxycinnamaldehyde (BCA), one of HCA derivatives, have antiproliferative activities on several human cancer cell lines. Our previous study suggested that reactive oxygen species (ROS) and caspase-3 are the major regulators of HCA-induced apoptosis. In the present study, we demonstrated a novel molecular target using *in vitro* pull-down assay by biotin-labeled HCA (biotin-HCA) in SW620 cells. We analyzed 11 differential spots of 2-dimensional gel prepared with pull-downed proteins by biotin-HCA. Among them, five spots were identified as proteasome subunits. An *in vitro* 26S proteasome function assay using specific fluorogenic substrates showed that HCA potently inhibits L3-like activity of the proteasome. In addition, HCA showed inhibitory action against chymotrypsin-like, trypsin-like, and PGPH-like activities. DNA microarray showed that HCA induced heat shock family and ER stress-responsive genes, which reflects the accumulation of misfolded proteins by proteasome inhibition. On western blot analysis, it was confirmed that HCA induces glucose-regulated protein, 78 kDa (GRP78) and some representative endoplasmic reticulum (ER) stress-responsive proteins. Furthermore, HCA treatment decreased mitochondrial membrane potential. The effect of HCA on cytochrome c and Bax translocation between cytosol and mitochondrial membrane was clarified using western blot analysis. These results suggest that HCA-induced apoptosis is associated with the inhibition of the proteasome activity that leads in turn to the increase of ER stress and mitochondrial perturbation.

* *Corresponding author*. Tel.: +82 42 860 4557; fax: +82 42 861 2675.
** *Corresponding author*. Tel.: +82 42 860 4568.
E-mail addresses: dchan@kribb.re.kr (D.C. Han), kwonbm@kribb.re.kr (B.-M. Kwon).

Abbreviations: HCA, 2′-hydroxycinnamaldehyde; BCA, 2′-benzoyl-oxycinnamaldehyde; ROS, reactive oxygen species; MCA, 4-methyl-coumaryl-7-amide; HMOX1, heme oxygenase 1; HERPUD1, homocysteine-inducible, endoplasmic reticulum stress-inducible, ubiquitin-like domain member 1; GADD153/CHOP, growth arrest and DNA damage-inducible gene/C/EBP homologous protein; GRP78, glucose-regulated protein, 78 kDa

0006-2952/$ – see front matter
doi:10.1016/j.bcp.2007.05.016

1. Introduction

2′-Hydroxycinnamaldehyde (HCA) and 2′-benzoyloxycinnamaldehyde (BCA), one of HCA derivatives, were reported to have various inhibitory activities such as anti-angiogenic [1], anti-inflammatory [2], anti-CDK4/cyclinD1 kinase [3], and anti-proliferation of several human cancer cells including breast, leukemia, ovarian, lung, and colon tumor [4]. Our previous study showed that BCA/HCA induce apoptosis of cancer cells mainly through elevation of reactive oxygen species (ROS) and caspase-3 activation [5]. BCA significantly blocks tumor growth in a nude mouse assay without body weight loss, demonstrating as a good drug candidate for cancer therapy [5]. However, the precise mechanism including the direct upstream proteins is not yet fully understood.

Searching for proteins with high affinity to BCA/HCA is very important to understand the molecular and biochemical mechanisms of their antiproliferative activities. Mass spectrometry-based proteomic analysis would be a powerful tool to identify proteins that bind to BCA/HCA. In the present study, we used biotin-labeled HCA (biotin-HCA) to identify their direct upstream proteins in SW620 colon cancer cells. MALDI-TOF analysis showed that biotin-HCA binds preferentially to proteasome subunits, and *in vitro* proteasome assay revealed that HCA has inhibitory activity on 26S proteasome function.

The ubiquitin-proteasome pathway is the major proteolytic system in the cytosol and nucleus of all eukaryotic cells. Introduction of proteasome inhibitors demonstrated that the proteasome catalyzes the degradation of a large variety of cellular proteins and is essential for the development of a number of major human diseases [6]. The ability of proteasome inhibitors to inhibit cell proliferation and selectively induce apoptosis in proliferating cells, together with their ability to inhibit angiogenesis [7,8], make them attractive candidates as anticancer drugs.

PS-341, one of representative proteasome inhibitors, has been known to induce apoptosis through inhibition of NF-κB and caspase activation [9]. However, endoplasmic reticulum (ER) stress and ROS were proved to be more sufficient to initiate apoptosis in HNSCC cells [10]. In the ER-Golgi complex, native proteins are folded into their proper tertiary structures, however, misfolded proteins are degraded by the 26S proteasome. Therefore, the inhibition of the 26S proteasome may increase the accumulation of misfolded proteins, resulting in ER stress [10]. Previous studies indicated that a group of stress-related genes was rapidly induced by PS-341 stimulation in cancer cells that were similar to the gene expression profile induced by ER stress. In the present study, we analyzed the induced genes after of HCA treatment using cDNA microarray and this revealed significant induction of a panel of genes, coding proteins implicated in ER stress, unfolded proteins, and protein folding.

Our previous study showed that HCA induced the expression of the proapoptotic proteins such as Bax [11], a mammalian cell death protein that targets mitochondrial membranes and can induce mitochondrial damage and cell death [12]. Furthermore, disruption of the mitochondrial membrane potential ($\Delta\psi_m$) was induced in cancer cells by various proteasome inhibitors [13]. On investigation of $\Delta\psi_m$, it could be shown that, the mitochondrial membrane potential was decreased upon HCA treatment. HCA also caused the release of mitochondrial cytochrome c to cytosol, and in contrast, translocation of Bax from cytosol to membrane, which are representative features during mitochondrial apoptotic pathway. Taken together, these results suggest that proteasome inhibition by HCA treatment caused ER stress and mitochondrial perturbation, and these are associated with apoptosis induction in cancer cells.

2. Materials and methods

2.1. Cell cultures

The SW620 colon cancer cells were grown in Dulbecco's modified Eagle's medium (DMEM) (GibcoBRL, Carlsbad, CA), supplemented with 10% fetal bovine serum (FBS) (GibcoBRL), 100 U/ml penicillin, and 100 μg/ml streptomycin (GibcoBRL). Cells were incubated at 37 °C in a 5% CO_2 humidified atmosphere.

2.2. Synthesis and identification of biotin-2′-hydroxycinnamaldehyde (biotin-HCA).

Ninety milligrams (0.36 mM) of biotin, 72 mg of DCC, 6 mg of DMAP were dissolved in DMSO, to which 45 mg (0.3 mM) of 2′-hydroxycinnamaldehyde was added. The reaction mixture was stirred for 2 h at room temperature. The reaction solution was concentrated and purified by silica gel column chromatography and HPLC to give 23 mg of 2′-biotinyl-O-cinnamaldehyde (biotin-HCA). ^{1}H NMR (MeOH-d_4) δ 9.67 (d, J = 7.5 Hz, 1H), 7.80 (dd, J = 2.1, 8.1 Hz, 1H), 7.70 (d, J = 16.2 Hz, 1H), 7.50 (dt, J = 1.2, 8.1 Hz, 1H), 7.33 (dt, J = 2.1, 8.1 Hz, 1H), 7.18 (dd, J = 1.2, 8.1 Hz, 1H), 6.78 (dd, J = 7.5, 16.2 Hz, 1H), 4.47 (m, 1H), 4.32 (m, 1H), 3.25 (m, 1H), 2.93 (m, 1H), 2.74 (m, 3H), 1.82-1.54 (m, 6H).

The IC_{50} value of antitumor acitivty for synthesized biotin-HCA was similar (30 μM) with that of HCA against SW620.

2.3. In vitro pull-down assay with biotin-HCA

In vitro pull-down with biotin-HCA was performed according to Hinck et al. [14] with several modifications. Cells were rinsed in PBS and solublized in CSK buffer (50 mM NaC1, 10 mM Pipes (pH 6.8), 3 mM $MgCI_2$, 0.5% Triton X-100, 300 mM sucrose, 1 mM PMSF, and 10 μg /ml leupeptin) for 20 min at 4 °C. Cells were scraped from the plates with a rubber policeman and sedimented in a centrifuge for 10 min. The soluble supernatant was collected and monomeric avidin (Pierce Chemical Co., Rockford, IL) was added for removing the nonspecific binding proteins to avidin. Fifty-micrometer of biotin-HCA was preincubated with avidin for 1 h at 4 °C and an equal volume of DMSO vehicle was incubated with avidin as a negative control. These two slurry fractions were added to the soluble protein fractions respectively, and incubated for 2 h at 4 °C. The samples were washed with PBS for three times, and finally eluted with 2 ml of 0.1 M glycine buffer. Eluted fractions were concentrated with Centricon YM-3 (cut-off 3000 Da, Millipore, Bedford, MA) to 100–150 μl, followed by a determination of protein concentration using a Bradford protein assay kit (Bio-Rad, Hercules, CA).

2.4. 2-Dimensional gel electrophoresis (2-DGE) and MALDI-TOF analysis

Forty-microgram proteins were solublized in rehydration sample buffer (8 M urea, 2% CHAPS, 50 mM DTT, 0.5 % IPG buffer, bromophenol blue) and applied onto 7 cm IPG strips (pH 4–7). IEF was performed from pH 4–7 carrying ampholytes at 8,750 v/h. After equilibrating in equilibration buffer (125 mM Tris–HCl (pH 6.8), 10% glycerol, 2% SDS, 1% DTT, bromophenol blue), the first-dimension gel was loaded onto the 12% acrylamide second-dimension gel. After separation, gels were silver-stained by a modified silver-staining method and the protein spots were compared.

For identification of the differentially detected spots from biotin-HCA by mass spectrometry, excised protein spots from silver-stained gels were destained for 5 min in 15 mM potassium ferricyanide and 50 mM sodium thiosulfate. After three washes with water, the gel pieces were dehydrated in 100% acetonitrile for 1 min and were then dried. Digestion was performed by the addition of 100 ng of trypsin (Promega, Madison, WI) in 200 mM ammonium bicarbonate. After enzymatic digestion overnight at 37 °C, the peptides were extracted twice with 50 μl of 60% acetonitrile /1% trifluoroacetic acid. Followed by the removal of acetonitrile via vacuum centrifugation, the peptides were concentrated using pipette tips C18 (Millipore, Billerica, MA) and identified by matrix-assisted laser-desorption ionisation – time-of-flight (MALDI-TOF) MS with a Voyager-DE STR instrument (PE-Biosystems, Waltham, MA) using angiotensin I and ACTH as standards. The acquired spectra were processed and searched against a MS-Fit database.

2.5. In vitro inhibition assay of 26S proteasome in whole cell extracts

Proteasome function was measured as previously described [15,16] with some modifications. Briefly, cells were washed with PBS, then with buffer I (50 mM Tris–HCl (pH 7.4), 2 mM DTT, 5 mM $MgCl_2$), and pelleted by centrifugation. Homogenization buffer (50 mM Tris–HCl, pH 7.4, 1 mM DTT, 5 mM $MgCl_2$, 250 mM sucrose) and glass beads (0.5 mm) were added and cells were vortexed for 2 min. Beads and cell debris were removed by centrifugation at 1000 × *g* for 5 min, followed by centrifugation at 10,000 × *g* for 20 min. Protein concentration was determined and 20 μg of protein from each sample were diluted with buffer I to a final volume of 200 μl. After addition of HCA, samples were incubated at R.T. for 1 h. The substrates for proteasome were dissolved in DMSO and added to a final concentration of 80 μM (1% DMSO). Total reaction mixtures were incubated at 37 °C for 1 h. The fluorogenic proteasome substrates Suc-LLVY-4-methyl-coumaryl-7-amide (MCA) (for chymotrypsin-like activity), Boc-VLK-MCA (for trypsin-like activity), Z-LLE-MCA (for PGPH-like activity), and Z-LLL-MCA (for L3-like activity) were purchased from Peptide Institute, Japan. Proteolytic activity was monitored by releasing the fluorescent group 4-methyl-coumaryl-7-amide (MCA) measured in a fluorescence plate reader (FLUOSTAR OPTIMA, BMG LABTECH, Offenburg, Germany) at 355/460 nm.

2.6. Microarray procedure

DNA microarray analyses were performed according to the manufacturer's standard protocol. Briefly, Cy3- or Cy5-dUTP labeled cDNA probes were prepared from 100 μg of total RNA isolated from the DMSO- or HCA-treated SW620 cells for 3 h. Different fluorescent-labeled probes from different cells were mixed and applied to a microarray following incubation at 65 °C overnight under humidified conditions. To control the labeling differences, duplicated reactions were carried out in which the fluorescent dyes were switched during synthesis. The fluorescent images of hybridized microarrays were scanned with a fluorescence laser confocal slide scanner (ScanArray 5000, GMI, Inc., Ramsey, MI). The original value of each spot was normalized by the values of all spots (global normalization) and/or house keeping genes and blank (buffer) spots on the slides. The fluorescence intensities of Cy3 and Cy5 were analyzed by the ImaGene 5.5 software (BioDiscovery Inc., El Segundo, CA). The log ratios of Cy5:Cy3 and clustering analysis were calculated by the GeneSight 3.5 software (BioDiscovery Inc.).

2.7. Western blot analysis

After transfer, PVDF membranes were incubated with a blocking buffer consisting of 10 mM Tris–HCl (pH 7.5), 50 mM NaCl, 1.8–5% nonfat dry milk, and 0.1% Tween 20 for 2 h. The membranes were then incubated for 1.5 to 3 h at room temperature with primary antibody. After three washes with washing buffer (Tris–buffered saline containing 0.1% Tween 20), the membranes were incubated with horseradish peroxidase-conjugated sheep antimouse or antirabbit IgG antibodies (Amersham Biosciences, Piscataway, NJ) at a dilution of 1:5000 for 30 min at room temperature. Immunodetection was accomplished by enhanced chemiluminescence (Amersham Biosciences) followed by autoradiography. Antibodies were purchased from the following sources: homocysteine-inducible, endoplasmic reticulum stress-inducible, ubiquitin-like domain member 1 (HERPUD1), growth arrest and DNA damage-inducible gene (GADD153), and heme oxygenase 1 (HMOX1) from Abvona (Taipei, Taiwan), glucose-regulated protein, 78 kDa (GRP78), cytochrome c, and Bax from BD Biosciences PharMigen (San Diego, CA).

2.8. Changes in mitochondrial membrane potential

$\Delta\psi_m$ was measured using a lipophilic cationic probe, 5,5′,6,6′-tetrachloro-1,1′,3,3′-tetraethyl-benzimidazolcarbo-cyanine iodide (JC-1). After incubating cells (10,000/well) in a 96-well plate with 0–30 μM of HCA for 1 to 12 h, cells were stained with 10 μg/ml JC-1 at 37 °C for 10 min. JC-1 detects a decrease in mitochondrial membrane potential, which fluoresces green. However, at high concentrations, aggregation occurs and both the absorption and emission spectra shifts to a longer wavelength, which fluoresces red. In cells, aggregate formation increases linearly with increasing membrane potential. A 485 nm filter was used in the fluorescence microplate reader for excitation of JC-1. In the first run of each plate, a 590 nm emission filter was used to detect a total orange fluorescence (JC-I aggregates) of the sample. A second run was performed on each plate with a 525 nm emission filter to detect green

fluorescence (JC-1 monomers). The relative ratio of A590 (red):A525 (green) was calculated as an indicator of mitochondrial potential. A decrease in membrane potential led to a decrease in the ratio of red to green fluorescence.

2.9. Subcellular fractionation for detection of cytochrome c and/or Bax translocation

Subcellular fractionation was performed as described previously [17] with several modifications. After treatment of 30 μM of HCA for 0 to 24 h, cells were pelleted, washed with cold-PBS and homogenized by passing the cell mixture through a 22-gauge needle in buffer (250 mM sucrose, 20 mM HEPES pH 7.4, 5 mM $MgCl_2$, 10 mM KCl, 1 mM EDTA, 1 mM EGTA) supplemented with protease inhibitor cocktail. Cytosolic (supernatant) and membrane (pellet) fractions were separated by centrifugation at 13,000 *g* for 10 min. Protein concentrations were determined by the Bradford assay and 30 μg protein are resolved by SDS-PAGE and immunoblotted for detection of cytochrome c and Bax.

3. Results

3.1. Identification of proteasome subunits as one of the high affinity proteins with HCA

We hypothesized that HCA mediates serial biological activities through its direct interaction with intracellular target protein(s). Therefore, we prepared the biotin-HCA for identification of the direct upstream protein (Fig. 1) and performed an *in vitro* affinity pull-down assay from the whole cell lysates of SW620 by biotin-HCA and DMSO vehicle, respectively. Some protein spots on 2-DGE were only detected by biotin-HCA (Fig. 2). These spots have been shown to interact specifically with biotin-HCA because pretreatment of cell lysates with an excess of monomeric avidin removed nonspecific binding to avidin. Eleven spots were cut from 2-DGE gel and were then digested with trypsin, followed by MALDI-TOF analysis for protein identification. From this study, 5 out of 11 protein spots were identified as proteasome subunits (Table 1). The other spots which showing matched molecular weights and pI values have been identified as ADP-ribosyl cyclase 1 or lipid phosphate phosphatase.

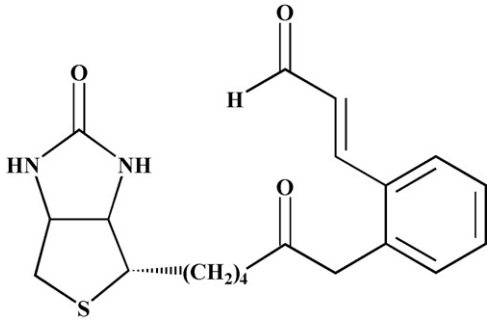

Fig. 1 – Structure of biotin-HCA.

3.2. Inhibition of 26S proteasome function in whole cell extracts

The identification of the major HCA-binding proteins as proteasome subunits suggested that HCA mediates antiproliferative effect via inhibition of proteasome function. To test this hypothesis, we performed *in vitro* assay for 26S proteasome function with whole cell extracts by using different fluorogenic proteasome substrates. Addition of HCA at concentration of 0–500 μM to whole cell lysates resulted in a dose-dependent inhibition of L3-like activity. Fifty-micrometer of HCA inhibited L3-like activity from 49.8% ± 0.02, chymotrypsin-like activity to 25% ± 0.01, trypsin-like activity to 33% ± 0.7, and PGPH-like activity to 20.1 ± 0.5 (Fig. 3).

3.3. Involvement of the ER stress in HCA-induced apoptosis

To see the genome-wide effects of HCA in cells, we analyzed the gene-expression profiles using DNA microarray upon treatment with 30 μM of HCA for 3 h in SW620 cells. According to our statistical analysis, as shown in Table 2, 28 genes were induced up to 2-fold by HCA treatment. These genes could be grouped according to their functions, which is in agreement with earlier reports for proteasome inhibitors: (i) Heat shock response genes [18]; (ii) A number of enzymes involved in amino acid metabolism [19]; (iii) ER stress-responsive genes such as GADD153, ATF3, HERPUD1, and HMOX1 [10]. These data indicated strongly that HCA-induced apoptosis is

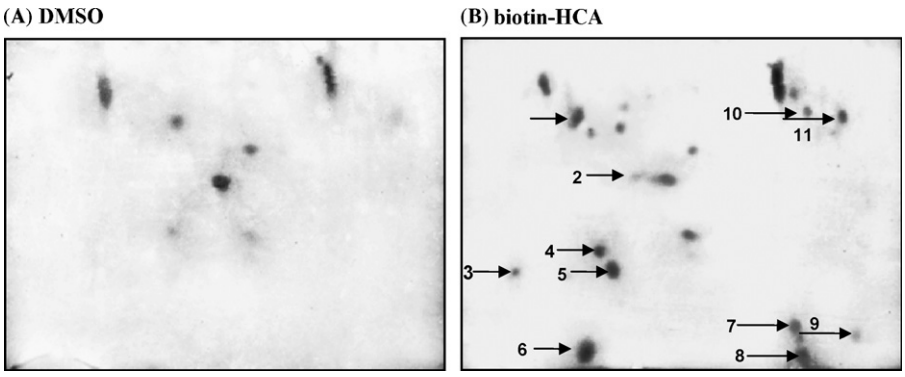

Fig. 2 – Silver-stained 2-DGE image of pull-downed proteins by DMSO vehicle (A), or biotin-HCA (B) in SW620 cells. Eleven spots specific to the 2-DGE image from biotin-HCA (B) were cut for Mass spectrometry analysis.

Table 1 – MALDI-TOF analysis of differentially pull-downed proteins by biotin-HCA

Spot No	Score	Covertion (%)	Mean error (ppm)	Protein MW (kDa)/pI	Protein name
3	679	17	7.25	29.2/5.7	Proteasome subunit beta type 4 precursor (EC 3.4.25.1) (Proteasome beta chain) (Macropain beta chain) (Multicatalytic endopeptidase complex beta chain) (Proteasome chain 3) (HSN3) (HsBPROS26)
5	187	13.7	0.01	29.6/6.1	Proteasome subunit alpha type 1 (EC 3.4.25.1) (Proteasome component C2) (Macropain subunit C2) (Multicatalytic endopeptidase complex subunit C2) (Proteasome nu chain) (30 kDa prosomal protein) (PROS-30)
6	140	14.4	6.82	29.2/5.7	Proteasome subunit beta type 4 precursor (EC 3.4.25.1) (proteasome beta chain) (macropain beta chain) (multicatalytic endopeptidase complex beta chain) (proteasome chain 3) (HSN3) (HsBPROS26)
7	140	14	−3.64	29.2/5.7	Proteasome subunit beta type 4 precursor (EC 3.4.25.1) (proteasome beta chain) (macropain beta chain) (multicatalytic endopeptidase complex beta chain) (proteasome chain 3) (HSN3) (HsBPROS26)
9	315	17.9	−0.83	29.6/6.1	Proteasome subunit alpha type 1 (EC 3.4.25.1) (proteasome component C2) (macropain subunit C2) (multicatalytic endopeptidase complex subunit C2) (proteasome nu chain) (30 kDa prosomal protein) (PROS-30)

associated with ER stress. Therefore, we investigated the expression or activation of some representative ER stress-responsive genes including GADD153, HMOX1, HERPUD1, and GRP78 by western blot analysis. As shown in Fig. 4, treatment of SW620 cells with HCA strongly induced GADD153, HMOX1, HERPUD1, and GRP78 genes as early as 3–8 h.

3.4. *Involvement of the mitochondrial apoptotic pathway by HCA treatment*

Our previous study showed that the antioxidant NAC significantly inhibited HCA-induced apoptosis [5]. It is well known that ROS generation is critical for apoptosis induction by proteasome inhibition through mediation of mitochondrial perturbation. Therefore, we hypothesized that HCA could induce perturbation of $\Delta\psi_m$ in cancer cells. We analyzed the decrease of the mitochondrial membrane potential by the reduction in the ratio of A590 (red):A520 (green). Thirty-micrometer of HCA treatment caused a gradual decrease of membrane potential after 2–4 h, and reached to 60% of the ratio after 12 h, indicating a significant reduction in mitochondrial membrane potential (Fig. 5).

The release of mitochondrial cytochrome c to cytosol, and in contrast, translocation of Bax from the cytosol to the membrane are representative features during mitochondrial apoptotic pathway. We therefore investigated whether

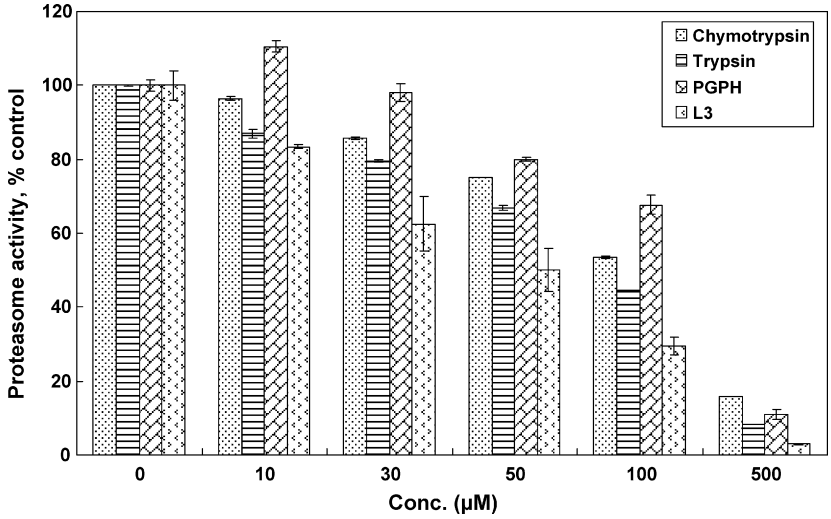

Fig. 3 – *In vitro* inhibitory effects of HCA on the chymotrypsin-like, trypsin-like, PGPH-like, and L3-like activity of 26S proteasome from whole cell extracts of SW620 cells. The released free MCA groups were measured and the relative activity was determined as a percentage of proteasome activity of the control. SW620 cell extract (20 μg/reaction) was incubated for 1 h with various fluorogenic peptide substrates for the proteasomal chymotrypsin-like, trypsin-like, PGPH-like, and L3-like activity. The results were derived from 3–4 independent experiments and each bar represents standard deviation.

Table 2 – Identification of HCA-induced genes by DNA microarray analysis

Gene ID	Fold change	Gene symbol	Title	Biological process
H200006965	7.9	DNAJB1	DnaJ homolog subfamily B member 1	Protein folding
H200001719	5.3	HSPA1B	Heat shock 70 kDa protein 1	
H300010702	4.6	HERPUD1	Homocysteine-responsive ER-resident ubiquitin-like domain member 1 protein	Response to unfolded protein
H300016699	4.1	ASNS	Asparagine synthetase	Asparagine biosynthesis
H200017080	4.0	HSPA1B	Heat shock 70 kDa protein 1	
H200000767	3.9	HSPA7	Heat shock 70 kDa protein 6	Protein folding
H200017926	3.9	SLC38A2	Amino acid transporter 2	Amino acid transport
H200014949	3.8	HMOX1	Heme oxygenase 1	Heme oxidation
H200019847	3.7	DDIT3	GADD153	
H300019008	3.6	HSPH1	Heat-shock protein 105 kDa	Protein folding
H200001314	3.2	ARHE	Rho-related GTP-binding protein RhoE	Protein transport
H200009481	3.1	HSPCA	Heat shock protein HSP 90-alpha	Mitochondrial transport; protein folding
H200002463	3.1	BAG3	BAG-family molecular chaperone regulator-3	Protein folding
H200004534	2.9	DNAJB4	DnaJ homolog subfamily B member 4	Protein folding
H300016001	2.9	HSPA1B	Heat shock cognate 71 kDa protein	Protein folding
H300005367	2.8	HSPCAL3	Heat shock protein 86	
H200020483	2.5	DNAJB6	DnaJ homolog subfamily B member 6	
H200014300	2.4	SLC7A5	Large neutral amino acids transporter small subunit 1	Amino acid metabolism
H200013986	2.4	MTHFD2	Bifunctional methylenetetrahydrofolate dehydrogenase/cyclohydrolase	Folic acid and derivative biosynthesis
H200006058	2.4	GARS	Glycyl-tRNA synthetase	Glycyl-tRNA aminoacylation
H300001138	2.4	AARS	Alanyl-tRNA synthetase	Alanyl-tRNA aminoacylation
H200013712	2.3	SUI1	Eukaryotic translation initiation factor 1	Protein biosynthesis; response to stress
H200010382	2.2	GCLM	Glutamate-cysteine ligase regulatory subunit	Cysteine metabolism
H300019036	2.2	DNAJA1	Heat shock 40 kDa protein 4	–
H300011906	2.2	SLC7A11	Cystine/glutamate transporter	Amino acid transport
H300005742	2.1	SLC1A4	Neutral amino acid transporter A	Dicarboxylic acid transport
H300018812	2.1	SLC16A6	Monocarboxylate transporter 7	Monocarboxylic acid transport
H300014542	2.0	DNAJA1	Heat shock 40 kDa protein 4	

cytochrome c and/or Bax translocate between the membrane and cytosolic fractions upon treatment with HCA using subcellular fractionation and western blot analysis. Fig. 6 shows that the level of cytochrome c was markedly increased in the cytosolic fraction as early as 8 h. Bax, on the contrary to cytochrome c, is remarkably increased at the membrane fraction with the concurrent decrease at cytosolic fraction by HCA treatment.

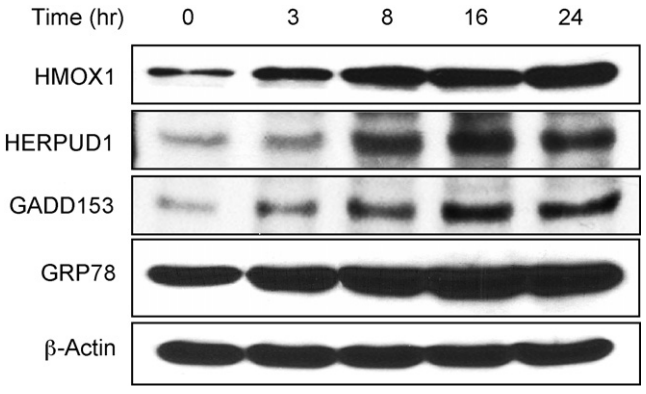

Fig. 4 – Protein expression of ER stress-responsive genes by HCA treatment. SW620 cells were treated with 30 μM of HCA for the indicated time periods, and the whole-cell extracts were prepared. Thirty-microgram aliquots of proteins were immunoblotted for each protein expression. ER stress-responsive proteins have been induced as early as 3–8 h. We performed these experiments three times for each antibody.

4. Discussion

HCA, isolated from an edible source, has been shown to exert an anti-tumor effect in a number of different cell types. In the present study, we demonstrated that proteasome is one of the direct upstream proteins for HCA-induced apoptotic death in cancer cells. HCA developed a G2/M cell cycle arrest in SW620 cells, associated with an increased expression of cyclin A and cyclin B1 [3], and decreased Bcl-2, and Bcl-X_L [5]. Our previous study to confirm the antiproliferative effects of HCA in cancer cells found to induce apoptosis mainly through the elevation of ROS [5]. In addition, BCA/HCA induced activation of caspase-3, degradation of poly(ADP-ribose) polymerase [5], and inhibited NF-κB activation in SW620 cells [11].

We hypothesized that HCA mediates its biological activity through its direct interaction with an intracellular protein(s). To identify this receptor(s), we synthesized a biotinylated HCA to serve as an affinity chromatography reagent. Avidin affinity column, 2-DGE, and MALDI-TOF analyses have shown that 5 of 11 differentially pull-downed spots by biotin-HCA are proteasome subunits. The 2-DGE image of these proteasome spots has been shown to be similar with part of previous image

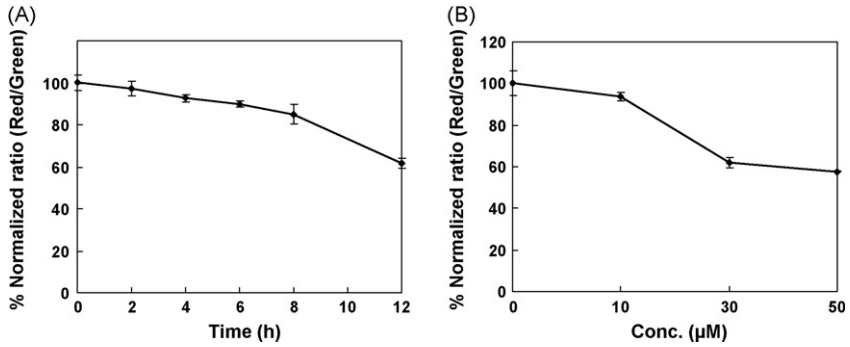

Fig. 5 – Perturbation of mitochondrial membrane potential by HCA treatment in SW620 cells. After incubating cells in a 96-well plate upon treatment with 30 μM of HCA for 1–12 h (A), and with 0–50 μM for 12 h (B), cells were stained with 10 μg/ml JC-1 at 37 °C for 10 min. $\Delta\psi_m$ in mitochondria can be followed by observing relative changes in the ratio of A_{590} (red):A_{520} (green). A reduction in this ratio indicates a decrease in membrane potential. This result is representative of three independent experiments and each bar represents standard deviation.

results [20]. Further studies are still required to reveal the precise interaction site(s) of proteasome with HCA using serial other methods such as LC-mass spectrometry or more detailed proteomic study.

The relative importance of the different proteolytic sites containing the chymotrypsin-like and the caspase- or trypsin-like sites in mammalian proteasome have been studied systematically [21]. This study showed that assaying the chymotrypsin-like activity overestimates the actual reduction in protein degradation and inhibition of multiple sites is required to markedly decrease proteolysis. Therefore, HCA assumed to be an effective proteasome inhibitor by inactivating multiple catalytic activities. A tripeptide aldehyde protease inhibitor, benzyloxycarbonyl (Z)-Leu-Leu-Leucinal (ZLLLal), initiates neurite outgrowth in PC12 cells at an optimal concentration of 30 nM [22]. This suggests the existence of a protease that regulates neurite formation in PC12 cells. Tsubuki et al. identified the target protease of ZLLLal in bovine brain using Z-Leu-Leu-Leu-MCA (ZLLL-MCA) as a proteasome with a molecular mass of about 660 kDa [22]. They also showed that the activity of the proteasome was inhibited efficiently by ZLLLal, and was different from the well known catalytic activities of proteasome in some aspects [23]. Pajonk et al. called this kind of proteasome activity L3-like [16]. The IC_{50} values of HCA for *in vitro* L3- and trypsin-like are 51 and 87 μM, respectively. The intracellular proteasome inhibition concentrations are assumed to be higher than these values.

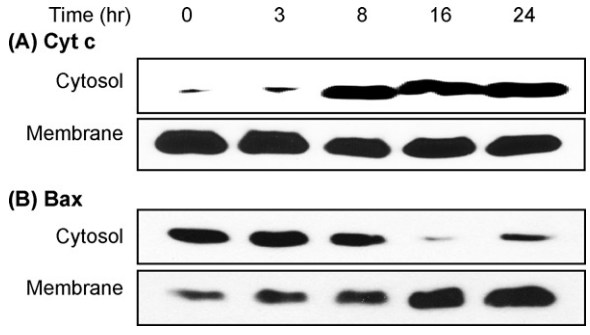

Fig. 6 – Cytochrome c and Bax translocation by HCA treatment. Cells were treated with 30 μM of HCA for the indicated time periods, and cytosolic and membrane fractions were generated as described in Section 2. Thirty-microgram aliquots of proteins were immunoblotted for cytochrome c (A) and Bax (B). Cytochrome c was released from membrane to cytosolic fraction whereas Bax was translocated from cytosolic to membrane fraction in response to HCA treatment.

Proteasome inhibitors cause apoptosis, since regulated proteolysis performs very important roles in various biochemical pathways including cell cycle control and gene expression regulation. The sequence of events leading to apoptosis following proteasome inhibition is suggested by Fribley et al [10], and Ling et al. [13]. They showed that ROS generation plays a critical role in the initiation of the PS-341-induced apoptotic cascade by mediation of ER stress and mitochondrial perturbation. However, it is not known how the inhibition of proteasome function can directly induce the ROS generation and the disruption of $\Delta\psi_m$.

Previous studies using DNA microarray showed that proteasome inhibitor treatment in human cancer cells induced heat shock genes, especially ER stress-responsive genes [10,24]. Ding Q. et al. determined the role of proteasome inhibition in oxidative stress toxicity and concluded that heat shock proteins may confer resistance to oxidative stress by preserving proteasome function and attenuating the toxicity of proteasome inhibition [25]. We therefore analyzed the induction levels of these genes using DNA microarray. Interestingly, many kinds of heat shock family members were induced after 3 h treatment with HCA. We also found that HMOX1, a regulator of reactive oxygen species; HERPUD1, a membrane protein induced by ER stress; growth arrest and DNA damage-inducible gene/C/EBP homologous protein (GADD153/CHOP) and ATF4, ER stress-dependent proteins [10], were also significantly induced by HCA treatment. Western blot analyses using antibodies against HERPUD1, GADD153, and HMOX1 also showed increased expression of these genes by HCA treatment. We further investigated one of

specific markers of ER stress, GRP78, by western blot analysis. GRP78 is a central regulator of ER function in the coordination of ER protein processing with mRNA translation during ER stress [26]. In the present study, GRP78 showed increased expression as early as 3 h treatment of HCA. Altogether, these data suggest that HCA-induced apoptosis is associated with ER stress in cancer cells. Fribley et al. showed that the addition of antioxidant abrogated the accumulation of ER stress-responsive genes, suggesting that ROS might play a role in ER stress mediated gene expression [10]. Therefore, it needs to be investigated whether antioxidant abolishes ER stress-induced gene expression by HCA treatment.

It has been reported that the release of cytochrome c is the critical molecular event for the apoptotic cascade [27]. The precise mechanism by which cytochrome c is released from the mitochondrial membrane space remains unclear. However, it has been known that Bax can directly induce the release of cytochrome c from the mitochondria [28]. Our previous study showed the induction of Bax protein by HCA treatment in cancer cells [11]. Therefore, we analyzed the participation of the mitochondria on HCA-induced apoptosis. In the present study, mitochondrial membrane potential was decreased by HCA treatment. Cytochrome c was also released from membrane to cytosolic fraction as early as 8 h after HCA treatment, which is in agreement with earlier reports in gastric cancer [29]. Furthermore, Bax translocation from cytosolic to membrane fraction increased gradually after HCA treatment. From these results, the mitochondrial perturbation is most likely to be part of the apoptotic cascade of events by HCA treatment. Ling et al. assayed the consequent events after treatment of superoxide scavenger to show the relationship between ROS generation and apoptosis induction by proteasome inhibition [13]. They reported that superoxide scavenger abrogated ROS generation and mitochondrial perturbation, suggesting that ROS generation plays a critical role in the initiation of the apoptotic cascade by mediation of the mitochondrial perturbation. We are investigating which kind of ROS is critical for apoptosis induction by HCA treatment, and the cascade reaction after inhibiting ROS generation. It would be ultimately worth investigating how the inhibition of proteasome function can induce the ROS generation.

More recently, it has been known that at least two different mechanisms have been associated with ER stress-initiated apoptosis, that is the unfolded protein response and disregulation of Ca^{2+} homeostasis [30]. In most cell types, ER is the primary intracellular store of Ca^{2+}, where it participates in the folding, modification, and sorting of newly synthesized proteins. Previous work identified that an increase in cytosolic Ca^{2+} is associated with apoptosis, and disregulation of intracellular Ca^{2+} was among the first hallmarks of apoptosis [31]. Therefore, further studies are necessary to determine the change of Ca^{2+} concentration in cytosol for better understanding about HCA-induced apoptotic pathway in cancer cells.

Our unpublished data showed that BCA/HCA induces apoptosis only in cancer cells and there is almost no change of cell cycle profile in normal cells. In general, proteasome inhibitors induce apoptosis only in cancer cell lines, which is even more resistant to apoptosis, due to mutations in some components of the apoptotic machinery such as p53 [32]. More precise explanations about the mechanisms are needed, but it is well known that the mutant proteins in cancer cells are highly unstable compared to the wild type and are rapidly degraded through the ubiquitin-proteasome pathway [33,34]. Therefore, cancer cells could be more sensitive to proteasome inhibitors than normal cells, which is why proteasome inhibitors would be one of attractive drug candidates for cancer treatment.

Taken together, it could be concluded that HCA-induced apoptosis is associated with proteasome inhibition that leading in turn to the increase of ER stress and mitochondrial perturbation, which are representative events for apoptosis induction by proteasome inhibitors.

Acknowledgement

This work was supported by the Plant Diversity Research Center of the 21st Century Frontier Research Program, the National Chemical Genomics Research Program, and the KRIBB Research Initiative Program.

REFERENCES

[1] Kwon B, Lee SH, Cho YK, Bok SH, So SH, Youn MR, et al. Synthesis and biological activity of cinnamaldehydes as anbiogenesis inhibitors. Bioorg Med Chem Lett 1997;7:2473–6.
[2] Lee SH, Lee SY, Son DJ, Lee H, Yoo HS, Song S, et al. Inhibitory effect of 2′-hydroxycinnamaldehyde on nitric oxide production through inhibition of NF-kappa B activation in RAW 264.7 cells. Biochem Pharmacol 2005;69:791–9.
[3] Jeong HW, Han DC, Son KH, Han MY, Lim JS, Ha JH, et al. Antitumor effect of the cinnamaldehyde derivative CB403 through the arrest of cell cycle progression in the G2/M phase. Biochem Pharmacol 2003;65:1343–50.
[4] Lee CW, Hong DH, Han SB, Park SH, Kim HK, Kwon BM, et al. Inhibition of human tumor growth by 2′-hydroxy- and 2′-benzoyloxycinnamaldehydes. Planta Med 1999;65:263–6.
[5] Han DC, Lee MY, Shin KD, Jeon SB, Kim JM, Son KH, et al. 2′-Benzoyloxycinnamaldehyde induces apoptosis in human carcinoma via reactive oxygen species. J Biol Chem 2004;279:6911–20.
[6] Elliott PJ, Ross JS. The proteasome: a new target for novel drug therapies. Am J Clin Pathol 2001;116:637–46.
[7] Oikawa T, Sasaki T, Nakamura M, Shimamura M, Tanahashi N, Omura S, et al. The proteasome is involved in angiogenesis. Biochem Biophys Res Commun 1998; 246:243–8.
[8] Drexler HC, Risau W, Konerding MA. Inhibition of proteasome function induces programmed cell death in proliferating endothelial cells. FASEB J 2000;14:65–77.
[9] Sunwoo JB, Chen Z, Dong G, Yeh N, Crowl Bancroft C, Sausville E, et al. Novel proteasome inhibitor PS-341 inhibits activation of nuclear factor-kappa B, cell survival, tumor growth, and angiogenesis in squamous cell carcinoma. Clin Cancer Res 2001;7:1419–28.
[10] Fribley A, Zeng Q, Wang CY. Proteasome inhibitor PS-341 induces apoptosis through induction of endoplasmic reticulum stress-reactive oxygen species in head and neck squamous cell carcinoma cells. Mol Cell Biol 2004;24: 9695–704.

[11] Lee SH, Lee CW, Lee JW, Choi MS, Son DJ, Chung YB, et al. Induction of apoptotic cell death by 2′-hydroxycinnamaldehyde is involved with ERK-dependent inactivation of NF-kappaB in TNF-alpha-treated SW620 colon cancer cells. Biochem Pharmacol 2005;70:1147–57.
[12] Green DR, Reed JC. Mitochondria and apoptosis. Science 1998;281:1309–12.
[13] Ling YH, Liebes L, Zou Y, Perez-Soler R. Reactive oxygen species generation and mitochondrial dysfunction in the apoptotic response to Bortezomib, a novel proteasome inhibitor, in human H460 non-small cell lung cancer cells. J Biol Chem 2003;278:33714–23.
[14] Hinck L, Nathke IS, Papkoff J, Nelson WJ. Dynamics of cadherin/catenin complex formation: novel protein interactions and pathways of complex assembly. J Cell Biol 1994;125:1327–40.
[15] Glas R, Bogyo M, McMaster JS, Gaczynska M, Ploegh HL. A proteolytic system that compensates for loss of proteasome function. Nature 1998;392:618–22.
[16] Pajonk F, Riess K, Sommer A, McBride WH. N-acetyl-L-cysteine inhibits 26S proteasome function: implications for effects on NF-kappaB activation. Free Radic Biol Med 2002;32:536–43.
[17] Dewson G, Snowden RT, Almond JB, Dyer MJ, Cohen GM. Conformational change and mitochondrial translocation of Bax accompany proteasome inhibitor-induced apoptosis of chronic lymphocytic leukemic cells. Oncogene 2003;22:2643–54.
[18] Bush KT, Goldberg AL, Nigam SK. Proteasome inhibition leads to a heat-shock response, induction of endoplasmic reticulum chaperones, and thermotolerance. J Biol Chem 1997;272:9086–92.
[19] Zimmermann J, Erdmann D, Lalande I, Grossenbacher R, Noorani M, Furst P. Proteasome inhibitor induced gene expression profiles reveal overexpression of transcriptional regulators ATF3, GADD153 and MAD1. Oncogene 2000;19:2913–20.
[20] Kristensen P, Johnsen AH, Uerkvitz W, Tanaka K, Hendil KB. Human proteasome subunits from 2-dimensional gels identified by partial sequencing. Biochem Biophys Res Commun 1994;205:1785–9.
[21] Kisselev AF, Callard A, Goldberg AL. Importance of the different proteolytic sites of the proteasome and the efficacy of inhibitors varies with the protein substrate. J Biol Chem 2006;281:8582–90.
[22] Saito Y, Tsubuki S, Ito H, Kawashima S. The structure-function relationship between peptide aldehyde derivatives on initiation of neurite outgrowth in PC12h cells. Neurosci Lett 1990;120:1–4.
[23] Tsubuki S, Kawasaki H, Saito Y, Miyashita N, Inomata M, Kawashima S. Purification and characterization of a Z-Leu-Leu-Leu-MCA degrading protease expected to regulate neurite formation: a novel catalytic activity in proteasome. Biochem Biophys Res Commun 1993;196:1195–201.
[24] Lee DH, Goldberg AL. Proteasome inhibitors cause induction of heat shock proteins and trehalose, which together confer thermotolerance in Saccharomyces cerevisiae. Mol Cell Biol 1998;18:30–8.
[25] Ding Q, Keller JN. Proteasome inhibition in oxidative stress neurotoxicity: implications for heat shock proteins. J Neurochem 2001;77:1010–7.
[26] Little E, Ramakrishnan M, Roy B, Gazit G, Lee AS. The glucose-regulated proteins (GRP78 and GRP94): functions, gene regulation, and applications. Crit Rev Eukaryot Gene Expr 1994;4:1–18.
[27] Liu X, Kim CN, Yang J, Jemmerson R, Wang X. Induction of apoptotic program in cell-free extracts: requirement for dATP and cytochrome c. Cell 1996;86:147–57.
[28] Jurgensmeier JM, Xie Z, Deveraux Q, Ellerby L, Bredesen D, Reed JC. Bax directly induces release of cytochrome c from isolated mitochondria. Proc Natl Acad Sci USA 1998;95:4997–5002.
[29] Fan XM, Wong BC, Wang WP, Zhou XM, Cho CH, Yuen ST, et al. Inhibition of proteasome function induced apoptosis in gastric cancer. Int J Cancer 2001;93:481–8.
[30] Ferri KF, Kroemer G. Organelle-specific initiation of cell death pathways. Nat Cell Biol 2001;3:E255–63.
[31] Rizzuto R, Pinton P, Ferrari D, Chami M, Szabadkai G, Magalhaes PJ, et al. Calcium and apoptosis: facts and hypotheses. Oncogene 2003;22:8619–27.
[32] Soligo D, Servida F, Delia D, Fontanella E, Lamorte G, Caneva L, et al. The apoptogenic response of human myeloid leukaemia cell lines and of normal and malignant haematopoietic progenitor cells to the proteasome inhibitor PSI. Br J Haematol 2001;113:126–35.
[33] Maurice D, Pierreux CE, Howell M, Wilentz RE, Owen MJ, Hill CS. Loss of Smad4 function in pancreatic tumors: C-terminal truncation leads to decreased stability. J Biol Chem 2001;276:43175–81.
[34] Yaguchi H, Ohkura N, Takahashi M, Nagamura Y, Kitabayashi I, Tsukada T. Menin missense mutants associated with multiple endocrine neoplasia type 1 are rapidly degraded via the ubiquitin-proteasome pathway. Mol Cell Biol 2004;24:6569–80.